STUDIES IN NUCLEAR STRUCTURE AND BIG BANG NUCLEOSYNTHESIS USING PROTON BEAMS*

I. Mazumdar[a], M. Dhibar[b], S.P. Weppner[c], G. Anil Kumar[b]
A.K. Rhine Kumar[d], S.M. Patel[a], P.B. Chavan[a], C.D. Bagdia[a]
L.C. Tribedi[a]

[a]Tata Institute of Fundamental Research, Mumbai 400005, India
[b]Department of Physics, Indian Institute of Technology, Roorkee-247667, India
[c]Eckerd College, St. Petersburg, FL 33711, USA
[d]Department of Physics, Cochin University of Science and Technology
Cochin-682 022, India

(Received February 4, 2019)

We present the results of our measurements using proton beams to address two different problems, namely, inelastic scattering of proton by ^{12}C and radiative capture of proton by deuteron. The $^{12}\mathrm{C}(p,p'\gamma)^{12}\mathrm{C}$ reaction was carried out with proton-beam energies ranging from 8 to 22 MeV. The differential and total cross section of γ rays from the 4.438, 9.64, 12.7 and 15.1 MeV states were measured at all the beam energies and compared with detailed Optical Model calculations. We report, for the first time, the cross section and the branching ratio of the 9.64 MeV state. In a different experiment, cross sections and astrophysical $S(E)$ factors for $p+d$ capture reaction were measured for the first time at CM energies of 66, 116 and 166 keV. The measured values at these three new energies are found to be in good agreement with global set of data and in nice agreement with recent theoretical calculations.

DOI:10.5506/APhysPolB.50.377

1. Introduction

Studies in nuclear structure and reactions from low to medium and high energies have been dominated by heavy-ion probes for the last five decades. However, low-energy light-ion beams remain as relevant as they were before the advent of heavy-ion physics. Light-ion beams are essential for both nuclear structure and reaction studies. Light-ion induced capture reactions are one of the major tools for studies in nuclear astrophysics. We have embarked upon a programme to carry out in-depth studies in selected problems

* Presented at the Zakopane Conference on Nuclear Physics “Extremes of the Nuclear Landscape”, Zakopane, Poland, August 26–September 2, 2018.

relevant to nuclear structure and nuclear astrophysics. Here, we report on two recent measurements, namely, inelastic scattering of protons on ^{12}C and radiative proton capture of deuteron to produce ^{3}He. There are many compelling reasons to revisit the $^{12}\mathrm{C}(p,p'\gamma)^{12}\mathrm{C}$ reaction. It provides valuable insight about the exact structure (collective or single particle) of the excited states of ^{12}C. The role of α-particle clustering and the influence of giant resonance states in ^{12}C on its structural properties are also not fully well-understood. In addition, microscopic theories have been successful only for describing elastic channels and no calculation is available for $^{12}\mathrm{C}(p,p'\gamma)^{12}\mathrm{C}$ in the low-energy region below 40 MeV. On the experimental front, there exist very little data for this reaction for the 12.71 and 15.1 MeV states. While data for the cross section of the 9.64 MeV state are rather scarce, the branching ratio of the state has not been reported so far.

The radiative capture of proton on deuteron $d(p,\gamma)^{3}\mathrm{He}$ is a reaction of great importance both for nuclear astrophysics and few-body nuclear physics. As far as the nucleosynthesis of ^{3}He is concerned, the relevant beam energy varies from few keV to few hundred keV. Broadly, one can consider three scenarios for the production of ^{3}He (or depletion of deuteron) from $d(p,\gamma)^{3}\mathrm{He}$ reaction, namely, the Big Bang Nucleosynthesis (BBN), production in low-mass protostars, and production in low to medium mass stars like the Sun. The prevalent temperature in BBN (10^{9}K) translates to a beam energy of around few hundred keV for the $d(p,\gamma)^{3}\mathrm{He}$ reaction. The LUNA experiment [1] has provided high quality data for cross sections and astrophysical S-factors from 2.5 to 22 keV (CM), essentially covering the region of interest in stellar environment. However, there is rather limited data for the BBN energy region from 30 to 300 keV. It is quite evident from [2] that the experimental data are in disagreement with the best polynomial fit for S-factor and thereby introduce the uncertainty in the cross section in the range of 6–10% level. Our primary motivation was, therefore, to produce new data points in the energy range of 30 to 300 keV.

2. The $^{12}\mathrm{C}(p,p'\gamma)^{12}\mathrm{C}$ reaction

The $^{12}\mathrm{C}(p,p'\gamma)^{12}\mathrm{C}$ reaction was carried out by bombarding a mylar target of thickness 2.22 mg/cm^{2} with proton beam from the TIFR Pelletron accelerator. The beam energy was varied from 8 to 22 MeV. The gamma rays produced from the excited states of ^{12}C were detected using a $3.5'' \times 6''$ large volume cylindrical $\mathrm{LaBr_3}$:Ce detector [3]. The gamma angular distributions were measured at six different angles (60°, 75°, 90°, 105°, 120°, 135°) w.r.t. the beam direction by keeping the detector at a distance of 35 cm from the scattering chamber. The detector and portions of beam line facing the detector were well-shielded using lead bricks to reduce the background events. The beam was stopped on a Faraday cup beyond the target and total charge was measured using a beam current integrator.

The energy and timing signals from the detector were processed using standard NIM electronics. The shaped and amplified energy signal was recorded in a peak sensing ADC and data were collected in events mode. The timing signal from the anode of the PMT was fed to the Time-to-Amplitude converter (TAC) as a start signal and Pileup rejection was achieved using the zero-cross technique. Energy calibration of the detector was carried out using standard gamma sources, namely, ^{137}Cs (661.6 keV), ^{60}Co (1173, 1332 keV) and ^{22}Na (511, 1274 keV), and an Am–Be source for 4.44 MeV γ-rays. Typical γ-ray spectra of 4.4, 9.64, 12.7 and 15.1 MeV, for two different beam energies, are shown in figures 1 (a) and (b). It is worth noting that the present measurements using $LaBr_3$:Ce detector allow to obtain better quality spectra than those measured earlier using NaI(Tl) detector.

The background subtracted γ-ray yields were corrected for efficiencies of the detector to get the differential cross sections. The differential cross sections were fitted using Legendre polynomial functions as given below

$$\frac{\mathrm{d}\sigma}{\mathrm{d}\Omega} = \sum_{l=0;\ l=\mathrm{even}}^{l=l_{\max}} a_l P_l(\cos\theta) . \tag{1}$$

The total gamma cross section was obtained by integrating Eq. (1).

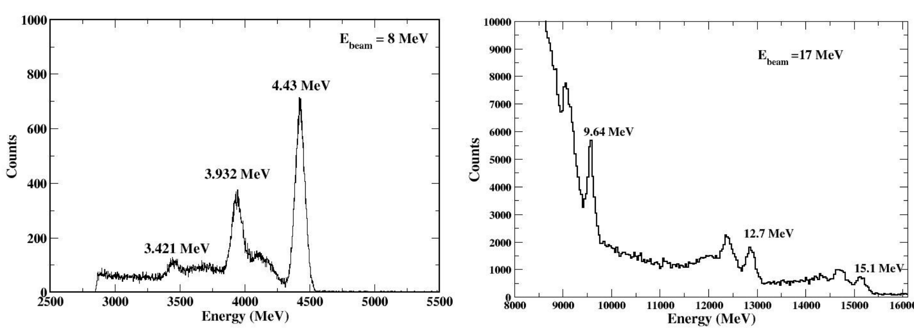

(a) (b)

Fig. 1. (a) γ spectrum for 4.43 MeV at $E_{\mathrm{beam}} = 8$ MeV. (b) γ spectrum for 9.64, 12.71 and 15.1 MeV at $E_{\mathrm{beam}} = 17$ MeV.

Figure 2 shows the experimentally extracted total cross sections for all the four states from 8 to 22 MeV.

We have carried out detailed theoretical analysis to understand and reproduce the experimental data, namely, angular distributions of the γ rays from the four states at all the beam energies and also the total (p, p')

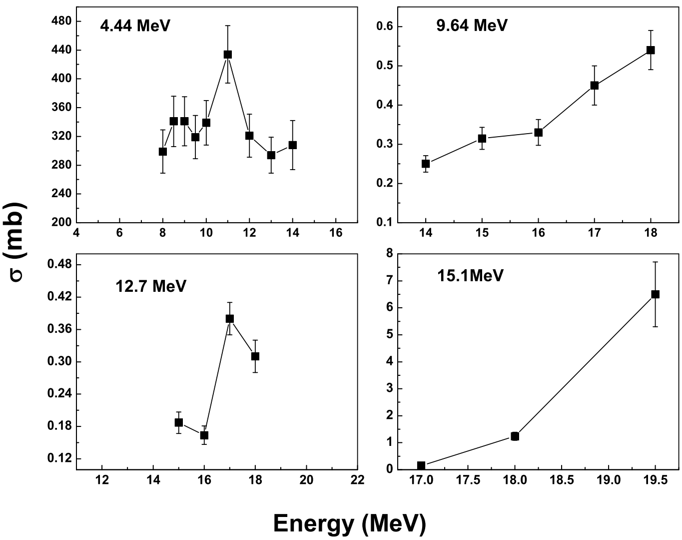

Fig. 2. Total cross sections for all the four states from 8 to 22 MeV.

cross sections. Traditionally, the analysis of the inelastic scattering process $(p, p'\gamma)$ is based upon either a microscopic theory of proton–nucleus interaction [4] or a phenomenological macroscopic approach. The macroscopic models treat the nucleus as a collective absorber and reflector of projectile current without explicit treatment of microscopic notions of antisymmetry, Pauli blocking and nucleonic degrees of freedom. These r-space phenomenological potentials are usually of the Woods–Saxon form and are easily entered in Distorted-Wave Born Approximation (DWBA) codes. We have analysed the data using both collective model and single particle excitation. The first step in the analysis involved determining the potential to be used for the calculations. We have generated a phenomenological optical model potential for proton or neutron on ^{12}C by fitting a very large body of experimental data for projectile energies ranging from 3 to 65 MeV [5]. The optical potential is of the Woods–Saxon form similar to that used in [6]. We have developed a DWBA code to fit the existing data for elastic scattering and total reaction cross sections for both proton and neutron. The results obtained from these calculations are fed into the code ECIS [7] for calculating the inelastic scattering cross sections for the four different excited states of ^{12}C. The calculations have been performed in two ways, (1) without considering coupling of states and (2) considering channel-coupling. The coupled-channel calculations have been done using ECIS considering six of the excited states of ^{12}C, namely, 4.43, 7.65, 9.64, 12.71, 15.11 and 16.11 MeV. In parallel with the collective model approach, there has been considerable effort to understand the excitation of ^{12}C using single particle model. We have augmented our original optical model potential using dispersion theory that constrains the single particle part of the real optical potential from the imaginary optical potential [8]. The single particle calculations have been carried out using our own code. The main purpose of this second line of attack is to provide us with an alternative beyond the phenomenological collective model. This approach is fundamentally microscopic in nature which allows a better understanding of the underlying mechanism generating the excited states. As inputs in these single particle calculations, we use the spectroscopic factors from shell model codes. The spectroscopic factor S details the strength of each single particle transition in making up the chosen excitation. We have considered the numbers from reference [9]. Figure 3 (a) shows the theoretical results for the partial $(p, p'\gamma)$ differential cross section of excitation to the 4.43 MeV (2^+) energy level along with the experimental data. The theoret-

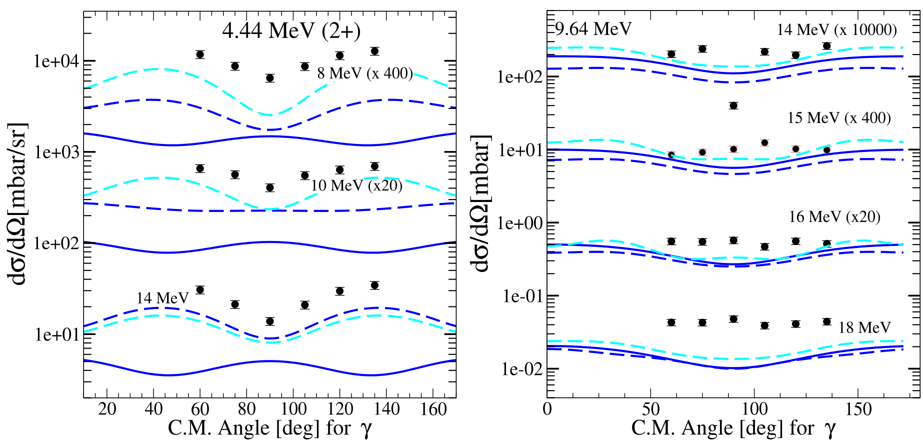

(a) (b)

Fig. 3. Theoretical reproduction of the differential cross sections for 4.44 MeV (a) and 9.64 MeV (b) at different beam energies. The different curves are with and without resonances.

ical results are from single particle model calculations. The dashed lines are calculations including the effect of resonances. The solid line does not include resonances. There is a strong influence of resonances in the excitation function of 4.4 MeV state. This typical structure of the excitation function is often used to verify ^{13}N resonances in a strong coupling model [10]. The existing data show a sharp rise in cross section at 8.3, 9.1, 10.5, 11.0, 12.7 and 13.8 MeV. Many of these are at the threshold of higher energy states in the ^{12}C nucleus. The dashed black/dark blue line represents the calculations considering resonances and the dashed grey/light blue line has also the Hoyle 2^+ state (9.85 MeV) added to it. Figure 4 shows the total cross-section for 4.44 MeV state. The experimental data are taken from literature and our present measurements (blue diamonds). The solid line is the single particle model calculation without adding resonances. The dashed black/dark blue line is after adding resonances and the dashed grey/light blue line also has the Hoyle 2^+ state added to it. Clearly, addition of the resonances brings in significant improvement in the reproduction of the data. Figure 3 (b) presents similar set of calculations for the 9.64 MeV state. For the lower beam energies (14 and 15 MeV), we obtain good agreement in terms of shape and magnitude of the data. At the highest energy of 18 MeV, the difference between theory and experiment is significant. This is because, for the 18 MeV beam energy, there may be some feeding from the higher states to the 9.64 MeV state through γ decay. This would enhance the measured cross-section of the 9.64 MeV γ rays. Unlike the 4.44 MeV state, the 9.64 MeV state is a large α emitter. The value of the γ branching ratio has not previously been reported. In this work, we have compared our measured γ cross section with the experimental (p, p') cross section [11] at 14 MeV beam energy. We have found the branching fraction to be 0.0035. We have compared our experimental data for the two higher states, namely, 12.71

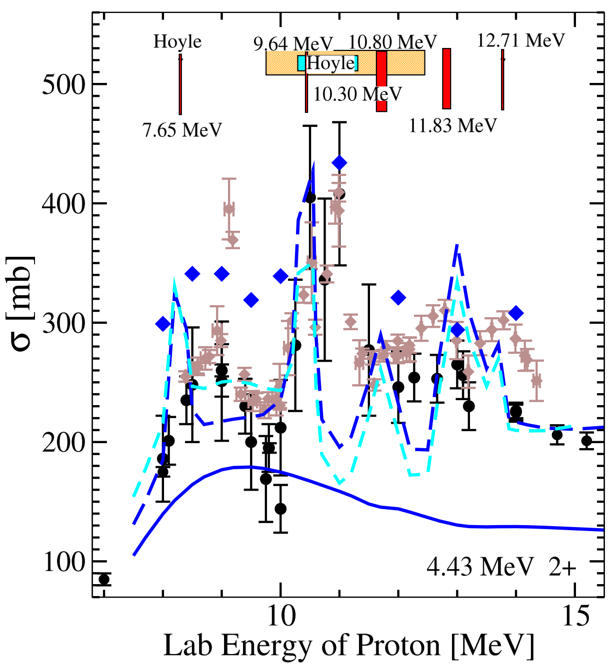

Fig. 4. Theoretical reproduction of the total cross sections for 4.44 MeV state using (p, p') reaction at different beam energies. The solid and dashed lines are calculations without and with resonances. The black/dark blue line considers the resonances and the grey/light blue line has also the Hoyle 2^+ state added to it.

and 15.1 MeV as well. We have concluded that while the 12.71 MeV data can be reproduced well with the calculations, there is no significant difference between the calculations with or without resonances. For the 15.1 MeV state, the calculated differential γ cross sections are significantly lower than the experimental value. This discrepancy is not fully understood and is currently under investigation.

3. The $d(p,\gamma)^3$He reaction

The $d(p,\gamma)^3$He reaction was carried out by bombarding a CD_2 target using proton beam of 100, 175 and 250 keV corresponding to CM energies of 66, 116 and 166 keV, respectively. The proton beam was obtained from the 14.5 GHz 300 W Electron Cyclotron Resonance (ECR) ion-source-based low energy accelerator facility at TIFR, Mumbai. The deuterated polyethylene (CD_2) target had thickness of 5.1×10^{17} atoms/cm^2. The γ rays produced from the capture of proton on deuteron were detected using the large volume $LaBr_3$:Ce detector, mentioned in previous section, at 4.5 cm from the centre of the target. The energy calibration was carried out using standard low-energy gamma sources, namely, ^{137}Cs (661.6 keV), ^{60}Co (1173, 1332 keV), ^{22}Na (511, 1274 keV). The γ rays of interest from the reaction for the beam energies of 100, 175 and 250 keV vary from 5.55 to 5.71 MeV. Therefore, an Am–Be source producing 4.433 MeV γ rays was also used for calibration, energy resolution and for determining the linearity of response up to 4.43 MeV. The detector had a very good linear response from 511 keV to 4.43 MeV. The beam was stopped on a Faraday cup beyond the target and was measured using a beam current integrator. The large volume detector was shielded from low-energy background radiation by $4''$ of lead shielding.

The astrophysical S-factor is defined as

$$S(E)_{\rm cm} = \frac{E_{\rm cm}\sigma(E)_{\rm cm}}{e^{-2\pi\eta}}\,, \tag{2}$$

where η denotes the Sommerfeld parameter and $2\pi\eta = 31.29\, Z_1\, Z_2(\mu/E)^{1/2}$, μ and E are the reduced mass of the system in amu and energy in c.m. system in keV.

Figure 5 presents the measured S-factors for 66, 116, 166 keV along with the other existing data from previous workers. Our measured values for both σ and S-factor are in good agreement with the global variation with energy. We have also found our measured values to be in excellent agreement with the recent calculations of Marcucci *et al.* [2]. Measurements at larger number of beam energies from 30 to 300 keV are currently ongoing and will be reported in future communications.

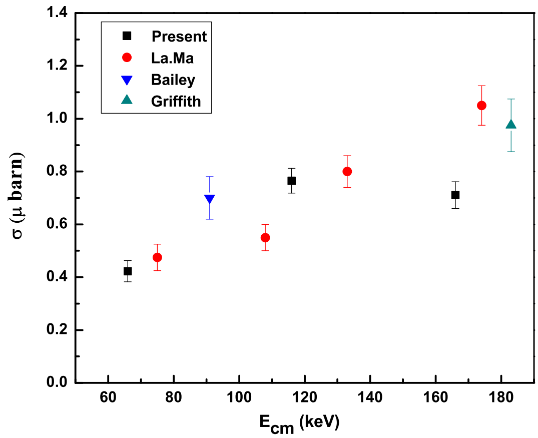

Fig. 5. Experimental $S(E)$ factors from the present and previous measurements.

4. Summary

We have carried out measurements of differential and total cross sections for four excited states of ^{12}C using $(p,p'\gamma)$ reaction from 8 to 22 MeV. We report, for the first time, the branching ratios of the 9.64 MeV state and the $(p,p'\gamma)$ reaction cross sections. Detailed coupled channel analysis using realistic Optical Model potentials has been performed to reproduce the data. The inclusion of different resonances is essential to reproduce the data. In a different experiment, we have measured the radiative capture cross sections and astrophysical S-factors of proton on deuteron at three new beam energies. The experimental values are in excellent agreement with very recent theoretical calculations.

REFERENCES

[1] C. Casella *et al.*, *Nucl. Phys. A* **706**, 203 (2002).

[2] L.E. Marcucci *et al.*, *Phys. Rev. Lett.* **116**, 102501 (2016).

[3] I. Mazumdar *et al.*, *Nucl. Instrum. Methods Phys. Res. A* **705**, 85 (2013).

[4] J.P. Jeukenne, A. Lejeune, C. Mahaux, *Phys. Rep.* **25**, 83 (1976).

[5] S.P. Weppner, private communication.

[6] S.P. Weppner *et al.*, *Phys. Rev. C* **80**, 034608 (2009).

[7] J. Raynal, ECIS-06, http://www.oecd-nea.org/tools/abstract/detail/nea-0850, 2006.

[8] W.H. Dickoff *et al.*, *J. Phys. G* **44**, 033001 (2017).

[9] B. Brown, *Prog. Part. Nucl. Phys.* **47**, 517 (2001) and references therein.

[10] F.C. Barker *et al.*, *Nucl. Phys.* **45**, 449 (1963).

[11] M. Harada *et al.*, *J. Nucl. Sci. Tech.* **36**, 313 (1999).